

VRR 00394

Temporal regulation of bovine coronavirus RNA synthesis

James G. Keck¹, Brenda G. Hogue², David A. Brian^{2*}
and Michael M.C. Lai¹

¹ *Departments of Microbiology and Neurology, University of Southern California, School of Medicine, Los Angeles, California, U.S.A. and* ² *Department of Microbiology, University of Tennessee, Knoxville, Tennessee, U.S.A.*

(Accepted for publication 9 November 1987)

Summary

The structure and synthesis of bovine coronavirus (BCV)-specific intracellular RNA were studied. A genome-size RNA and seven subgenomic RNAs with molecular weights of approximately 3.3×10^6 , 3.1×10^6 , 2.6×10^6 , 1.1×10^6 , 1.0×10^6 , 0.8×10^6 and 0.6×10^6 were detected. Comparisons of BCV intracellular RNAs with those of mouse hepatitis virus (MHV) demonstrated the presence of an additional RNA for BCV, species 2a, of 3.1×10^6 daltons. BCV RNAs contain a nested-set structure similar to that of other coronaviruses. This nested-set structure would suggest that the new RNA has a capacity to encode a protein of approximately 430 amino acids. Kinetic studies demonstrated that the synthesis of subgenomic mRNAs and genomic RNA are differentially regulated. At 4 to 8 h post-infection (p.i.), subgenomic RNAs are synthesized at a maximal rate and represent greater than 90% of the total viral RNA synthesized, whereas genome-size RNA accounts for only 7%. Later in infection, at 70 to 72 h p.i., genome-size RNA is much more abundant and accounts for 88% of total RNA synthesized. Immunoprecipitations of [³⁵S]methionine-pulse-labeled viral proteins demonstrated that viral protein synthesis occurs early in the infection, concurrent with the peak of viral subgenomic RNA synthesis. Western blot analysis suggests that these proteins are stable since the proteins are present at high level as late as 70 to 72 h p.i. The

Correspondence to: J.G. Keck, Depts. of Microbiology and Neurology, University of Southern California, School of Medicine, Los Angeles, CA 90033-1054, U.S.A.

* *Current address:* Department of Microbiology and Immunology, University of Southern California at Los Angeles, School of Medicine, Los Angeles, CA 90024, U.S.A.

kinetics of production of virus particles coincides with the synthesis of genomic RNA. These studies thus indicate that there is a differential temporal regulation of the synthesis of genomic RNA and subgenomic mRNAs, and that the synthesis of genomic RNA is the rate-limiting step regulating the production of virus particles.

Bovine coronavirus; Coronavirus; RNA

Introduction

The bovine coronavirus (BCV) is a hemagglutinating coronavirus that is antigenically related to the human respiratory coronavirus strain OC43 and the hemagglutinating encephalitis virus of swine, both of which hemagglutinate, and also to the mouse hepatitis virus (MHV), which has no hemagglutinating properties (Hogue et al., 1984; Hogue and Brian, 1986; King et al., 1985; Callebaut and Penseart, 1980). Hemagglutination by BCV appears to be the property of a fourth major structural protein, the hemagglutinin (King and Brian, 1982). Thus, BCV is comprised of four major structural proteins, a 190 kDa peplomeric protein (P or E2), (present on the virions as subunits of 120 and 100 kDa), a 140 kDa hemagglutinin protein (H or E3) (made up of two disulfide-linked subunits of 65 kDa), a 26 kDa matrix protein (M or E1), and a 52 kDa nucleocapsid protein (N). Because BCV has a significantly slower growth cycle than MHV, 48 to 72 h as compared to 12, BCV provides a potentially useful system to study the regulation of coronavirus RNA synthesis. The presence of a fourth structural protein also suggests that an additional mRNA species might be synthesized by BCV. Little is known about the molecular biology of BCV RNA synthesis.

All coronaviruses studied so far contain a positive-sense, single-stranded genome of $6-8 \times 10^6$ daltons (Lai and Stohlman, 1978; Lomniczi and Kennedy, 1977; Brian et al., 1980; Wege et al., 1978). In MHV, it has further been shown that, during virus replication, the viral genome is first transcribed into a full-length minus-strand template, which, in turn, is used as a template for transcribing genomic RNA and six subgenomic mRNAs (Lai et al., 1982; Leibowitz et al., 1981; Lai et al., 1981). The subgenomic mRNAs have a 3'-coterminal nested-set structure (Lai et al., 1981), with a leader sequence derived from the 5'-end of the genomic RNA (Lai et al., 1983, 1984; Spaan et al., 1983). The genome size RNA presumably serves two functions: one as the mRNA for translation of RNA polymerase(s) and the other as genomes to be packaged into progeny virus particles. No clear-cut structural features are known that can distinguish between the molecules serving these two functions. Perhaps the same molecule can serve both functions.

It has been shown with MHV and another coronavirus, avian infectious bronchitis virus (IBV), that the subgenomic mRNAs and genomic RNA are synthesized at the same rate throughout the viral replication cycle (Leibowitz et al., 1981; Stern and Kennedy, 1980). Thus, the relative ratio of all of the intracellular RNAs remains the same during infection. The viral genomic RNA gradually accumulates

throughout the infection. However, no clear-cut switching from transcription of subgenomic mRNAs to replication of genomic-sized RNA is seen. Thus, it is not known whether there is a temporal regulation of viral RNA synthesis in coronavirus-infected cells.

Since BCV has a longer growth cycle than that of MHV or IBV, BCV-infected cells offer a clear advantage for the study of temporal regulation of RNA transcription and replication, and protein synthesis. Our studies indicate that there is a differential regulation of transcription and replication of coronavirus RNA.

Materials and Methods

Viruses and cells

The Mebus strain of BCV was grown on Inaba bovine embryo kidney (BEK) cells, mouse L-2 cells or human adenocarcinoma cell line HRT-18 (King and Brian, 1982; Lai et al., 1981; Hogue et al., 1984). BCV stocks were prepared in BEK cells with virus grown no more than 20 passages beyond plaque purification (King and Brian, 1982). All cells were grown in Dulbecco's minimal essential medium (DMEM) supplemented with 10% fetal calf serum. Virus replication in BEK cells is mostly cell-associated, thus requiring three freeze-thaw cycles for virus release. The JHM strain of MHV was grown in DBT cells, a continuous murine astrocytoma line (Hirano et al., 1974), using the same medium as for BEK cells. Infection was carried out at a m.o.i. of approximately 1.

Plaque assay

BCV virus titers were determined using confluent monolayers of BEK cells in 60-mm dishes. Virus was serially diluted in serum-free DMEM, and 0.2 ml amounts of each dilution were applied to the monolayers. Virus was allowed to adsorb to cells for 3 h at 37°C. DMEM containing 1% fetal calf serum and 0.7% agarose was applied to the monolayers, and plaques were counted 3–4 days later.

Hemagglutination assay

This assay was performed in glass tubes using mouse erythrocytes which had been washed with phosphate buffered saline (PBS). Virus was serially diluted 2 fold with PBS and a 0.5% suspension of erythrocytes in PBS was added to each dilution. Virus-erythrocyte mixtures were incubated at room temperature overnight and titers were reported as the reciprocal of the highest virus dilution that gave a positive hemagglutination.

Radiolabeling and isolation of viral intracellular RNAs

Virus-infected cells at various time points post-infection (p.i.) were incubated with phosphate-free medium for 2 h. Actinomycin D was then added to a final

concentration of 2.5 $\mu\text{g}/\text{ml}$ 1 h prior to addition of [^{32}P]orthophosphate (250 $\mu\text{Ci}/\text{ml}$). After incubation with ^{32}P -medium for 2 h, the intracellular RNA was extracted according to the published procedure (Lai et al., 1981; Makino et al., 1984). Briefly, cells were lysed with 0.5% NP-40 and the nuclei were removed by centrifugation at $1000 \times g$ for 5 min. The supernatant fraction was made 1% final concentration with sodium dodecyl sulfate (SDS) and then extracted with an equal volume of 1:1 mixture of phenol (equilibrated with NTE buffer [10 mM Tris-HCl, pH 7.4, 100 mM NaCl, and 1 mM EDTA]) and chloroform. The RNA was precipitated with ethanol.

Agarose gel electrophoresis

RNA was denatured with glyoxal-DMSO and electrophoresed on 1% agarose gels as previously described by McMaster and Carmichael (1977). Gels were run at 16 mA overnight until the bromophenol blue dye had migrated to the bottom of the gel. The gels were then dried under vacuum and exposed to Kodak XAR-5 film with an intensifying screen.

Northern blot analysis

Intracellular RNA from virus-infected cells was denatured by glyoxal-DMSO treatment and then electrophoresed on 1% agarose gels made in 10 mM phosphate buffer, pH 7.0. After electrophoresis, the gel was transferred to Biotrans membrane filter by passive transfer using $20 \times \text{SSC}$ ($1 \times \text{SSC}$: 0.15 M NaCl and 0.015 M sodium citrate) for 24 h. The blots were baked at 80°C for 1 h. Pre-hybridization was performed for 1 h at 42°C in 50% formamide, 10 mM sodium phosphate (pH 6.5), $5 \times \text{SSC}$, $10 \times \text{Denhardt's}$ solution (0.2% each of bovine serum albumin, Ficoll and polyvinylpyrrolidone) and 125 $\mu\text{g}/\text{ml}$ salmon sperm DNA. Hybridization was done overnight in the same solution at 42°C using a nick-translated probe specific for the 3' end sequences of BCV genomic RNA. Two different probes were used. The first was the whole of the BCV clone pMN3, which encodes all of gene 7 and part of gene 6 (Lapps et al., 1987). The second probe was generated from clone pMN3 by digestion with *Xba*I and *Pst*I to generate a 1200-bp fragment. This fragment contains body sequences of gene 7 but not the poly A tail or the intergenic site between gene 6 and gene 7. The fragments were gel-purified and used for nick translation.

Radioisotopic labeling of intracellular viral polypeptides

BCV-infected cells were incubated with methionine-free medium containing 5% dialyzed fetal calf serum at various time points p.i., and [^{35}S]methionine (50 $\mu\text{Ci}/\text{ml}$) was added. After a 2 h labeling period, cells were washed with PBS and the proteins were solubilized using Laemmli sample buffer (Laemmli, 1970).

Polyacrylamide gel electrophoresis

SDS-polyacrylamide slab gel electrophoresis (SDS-PAGE) was performed as

described by Laemmli (Laemmli, 1970). The cell lysates extracted in Laemmli sample buffer were heated at 100°C for 3 min. After cooling, the lysates were electrophoresed on 7.5% polyacrylamide slab gels at 5 mA for 16 h. After electrophoresis, gels were treated for fluorography, dried and then exposed to Kodak XAR-5 film.

Protein immunoblot analysis

Proteins were electrophoretically transferred from SDS-PAGE gels to nitrocellulose paper for 16 h at 1 Amp. Blots were pre-incubated in a solution containing 10 mM Tris-HCl, pH 8.0, 150 mM NaCl, 1 mM disodium EDTA, 0.1% Triton X-100 and 3% bovine serum albumin and then incubated with a rabbit antibody prepared against the disrupted BCV virion particles (Hogue et al., 1984) in the same buffer at 4°C for 16 h. After incubation, blots were washed with the same buffer and then incubated with ¹²⁵I-labeled protein A. The washed blots were dried and then exposed to Kodak XAR-5 film.

Results

Characterization of BCV intracellular RNAs

MHV has been shown to synthesize six subgenomic mRNA species (Lai et al., 1981; Leibowitz et al., 1981). Since BCV is a close relative of MHV and contains an additional structural protein, the hemagglutinin, it was of interest to examine whether BCV synthesizes an additional mRNA species which may encode this structural protein. ³²P-labeled intracellular RNAs from BCV-infected cells were separated by agarose gel electrophoresis and compared to MHV intracellular RNAs (Fig. 1A). It was shown that BCV synthesizes seven subgenomic mRNA species, in contrast to six for MHV. The additional RNA species, designated 2a, lies between MHV mRNAs 2 and 3 and has a molecular weight of approximately 3.1×10^6 . The sizes of other RNAs are comparable between BCV and MHV except for mRNAs 4 and 5 of BCV, which are considerably smaller than the corresponding RNAs of MHV. The estimated sizes of these subgenomic mRNAs are 3.3×10^6 , 3.1×10^6 , 2.6×10^6 , 1.1×10^6 , 1.0×10^6 , 0.8×10^6 and 0.6×10^6 , respectively.

To confirm that these RNAs are indeed BCV-specific, intracellular RNAs from BCV-infected cells were separated by electrophoresis, transferred to a membrane filter and hybridized to a cDNA probe pMN3, representing the 3'-end 2.1 kb of the BCV genome (including the 3' noncoding region, all of the N gene and part of the M gene) (Lapps et al., 1987). This experiment presumes the 3'-coterminal nested set arrangement for BCV mRNAs. RNA patterns identical to those of in vivo labeled RNA species were obtained (Fig. 1B), confirming that all 7 subgenomic RNA species detected are BCV-specific RNAs. The abundance of genomic RNA was relatively low in this RNA preparation. However, longer exposure of the autoradiogram did show the presence of the genomic RNA (mRNA 1), the size of which is nearly identical to that of MHV (data not shown). The same RNA patterns were obtained from either BEK or L2 cells infected with BCV (data not shown).

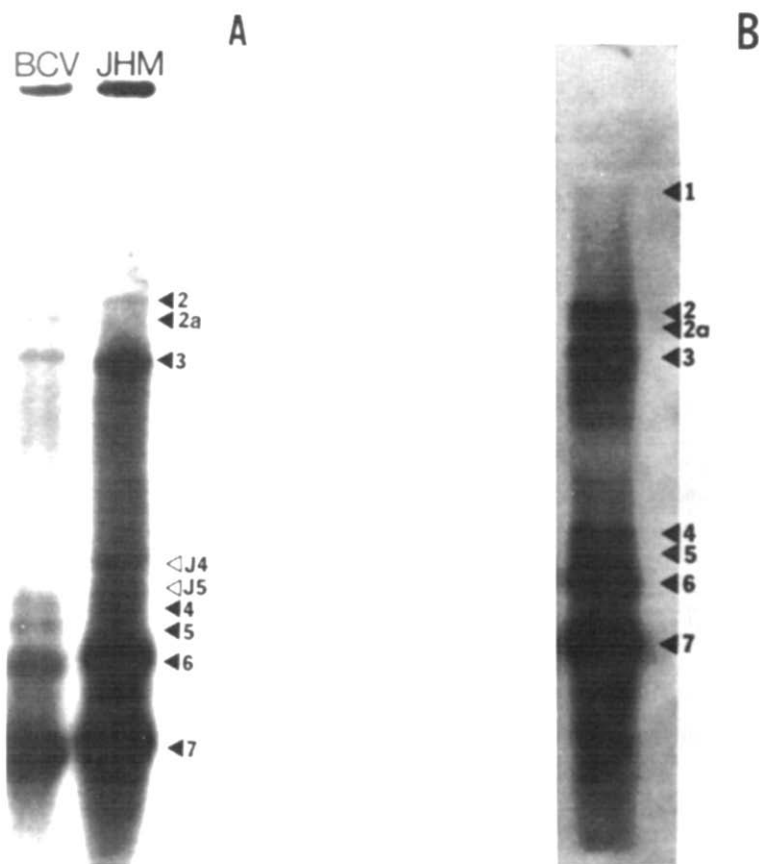


Fig. 1. Agarose gel electrophoresis of the virus-specific RNA in BCV-infected BEK and L2 cells. (A) BEK cells were pre-treated for 1 h with 2.5 $\mu\text{g}/\text{ml}$ Actinomycin D prior to labeling with [^{32}P]orthophosphate. Labeling was done from 2–4 h p.i. RNA was extracted, denatured with glyoxal–DMSO and electrophoresed on 1% agarose gels. For size comparison, ^{32}P -labeled JHM intracellular RNA was run in parallel. (B) Unlabeled BCV intracellular RNA extracted from L2 cells 24 h p.i. was separated by agarose gel electrophoresis, transferred to Biodyne paper and probed with a BCV-specific ^{32}P -labeled probe (see text).

To further demonstrate the 3′-coterminal nested-set structure, we used a cDNA probe representing 3′-end sequences only, that excluded the intergenic sequences and the poly A tail, to hybridize to BCV intracellular RNA. The same eight RNA species were detected (data not shown). This result established that all of the BCV RNA species contain 3′-overlapping sequences. The most likely explanation is that BCV RNAs also have a nested-set, 3′-coterminal structure, similar to other coronaviruses (Lai et al., 1981).

Temporal regulation of BCV RNA synthesis

To study whether RNA synthesis in BCV-infected cells is under temporal

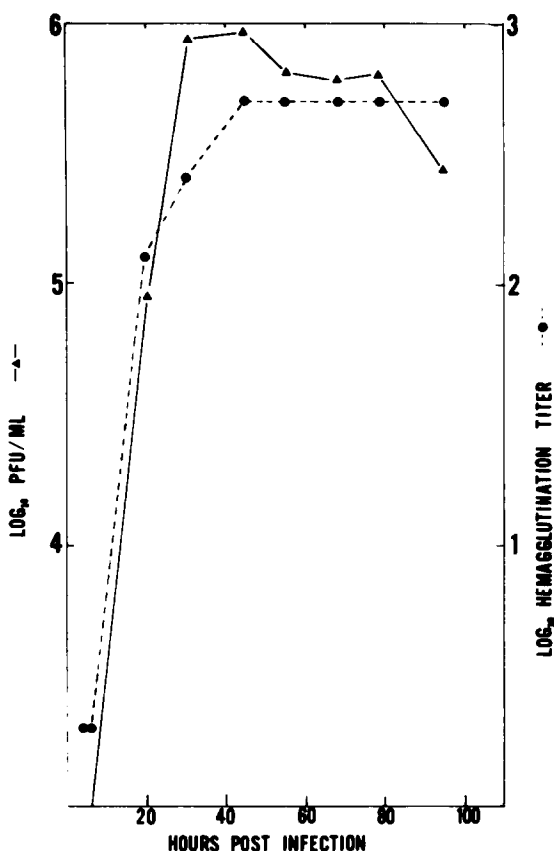


Fig. 2. Growth curve of BCV. BEK cells were infected with BCV at a m.o.i. of 1. Virus was harvested at appropriate time points by freeze-thawing the infected cells 3 times. Supernatants were assayed for virus titer by plaque assay and hemagglutination assay.

regulation, we first examined the kinetics of virus production. Maximum virus production from BCV-infected BEK cells was reached between 24 and 48 h p.i. as determined by plaque assay and hemagglutination titers (Fig. 2). Both assays gave identical growth curves. The virus continued to be produced through 96 h p.i. It should be noted that most of the mature virus was associated with infected cells and could only be released by repeated freezing and thawing of the infected cells.

To determine the kinetics of synthesis of various BCV-specific RNA species, the infected cells were labeled with [³²P]orthophosphate for 2 h at different time points p.i., and the intracellular RNA species were examined by agarose gel electrophoresis after denaturation with glyoxal-DMSO (Fig. 3A). At early time points after infection, all of the BCV-specific subgenomic mRNAs and genomic sized RNA were synthesized. The synthesis of subgenomic mRNAs was maximal between 6 and 8 h p.i., and gradually decreased. In contrast, the genome-sized RNA appeared to be a minor species early in the infection and gradually increased in its rate of synthesis at

later time. By 46 h p.i., genomic RNA was essentially the only RNA species synthesized. Very little subgenomic mRNA synthesis was detectable. The relative amounts of each RNA species synthesized at different time points were further quantitated by densitometry measurements and plotted in Fig. 3B. It can be seen that at 4–8 h p.i., the genome-size RNA constituted only 7% of the total viral RNAs synthesized. By 70–72 h p.i., as high as 88% of the total RNA synthesized was genomic RNA. The increase in the rate of the genomic RNA synthesis was accompanied by the concurrent decrease in the rate of subgenomic mRNA synthesis. The same conclusion is reached when the amounts of viral RNA synthesized are

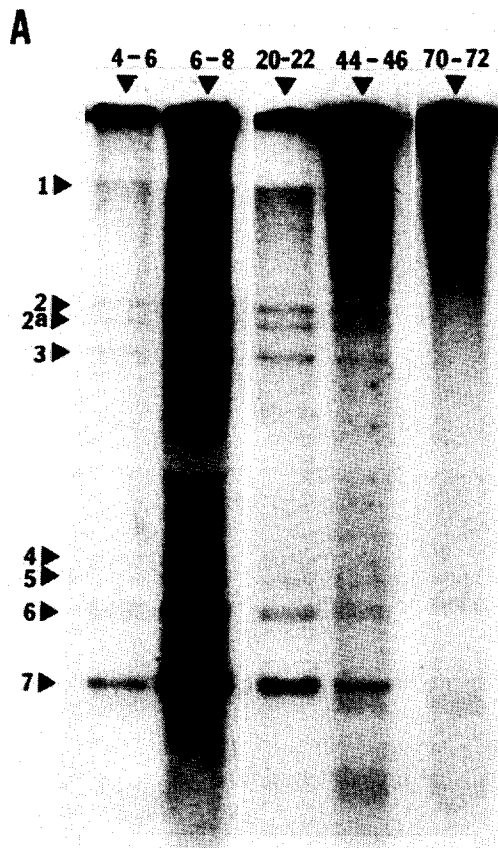


Fig. 3. Kinetics of viral RNA synthesis. BCV-infected cells were pretreated with 2.5 $\mu\text{g}/\text{ml}$ Actinomycin D for 1 h prior to labeling. Virus RNA was labeled at different time points using [^{32}P]orthophosphate for 2-h periods. (A) RNA was extracted, denatured with glyoxal–DMSO and electrophoresed on a 1% agarose gel. (B) A densitometer scan of viral RNA bands at each time point was used to determine the percentage of each viral RNA relative to the sum of densitometry values for all viral intracellular RNA. The percentage curve for each viral RNA is indicated by the following symbols: mRNA 1 (\blacktriangle), mRNA 2 (\blacksquare), mRNA 2a ($*$), mRNA 3 (\diamond), mRNA 4 (\blacklozenge), mRNA 5 (\circ), mRNA 6 (\triangle), and mRNA 7 (\bullet). (C) The same data were plotted as molar percentages of each RNA species relative to the total viral RNAs. The same symbols were used.

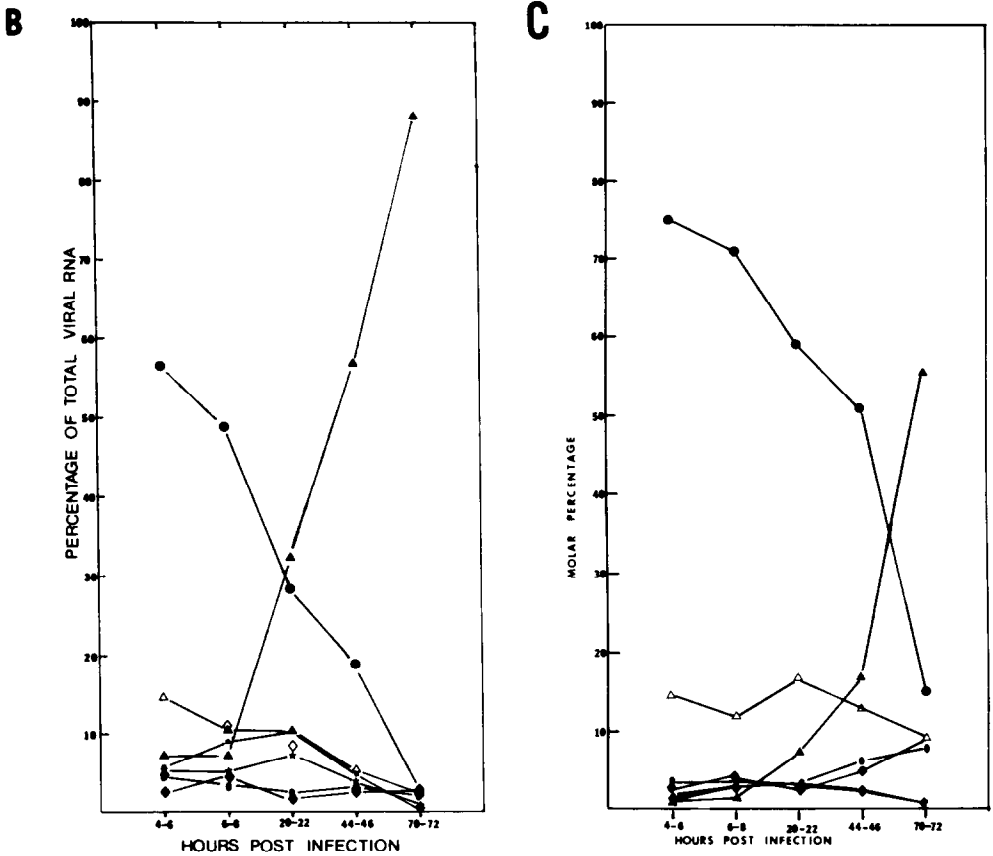


Fig. 3 (continued).

compared with respect to their molar ratios (Fig. 3C). Thus, there is an apparent switch of RNA synthesis from transcription of subgenomic RNA to the synthesis of genomic RNA.

Kinetics of viral structural protein synthesis

The data obtained above showed that the maximal rate of viral subgenomic mRNA synthesis occurred between 6–8 h p.i. while virus production did not reach maximal titers until 24–48 h p.i. Thus, it was of interest to determine when viral proteins were synthesized. BCV-infected cells were pulse-labeled with [35 S]methionine for 2-h periods beginning at different time points p.i., and viral proteins were immunoprecipitated with polyclonal antibodies specific for BCV and analyzed by polyacrylamide gel electrophoresis (Fig. 4). Although not all virus structural proteins could be identified, it is evident from the appearance of the two major protein species, N and M (E1), that the peak of viral protein synthesis took place between 4 and 8 h p.i., coinciding with the peak of subgenomic mRNA synthesis. The synthesis of M protein appears to be slightly later than that of N

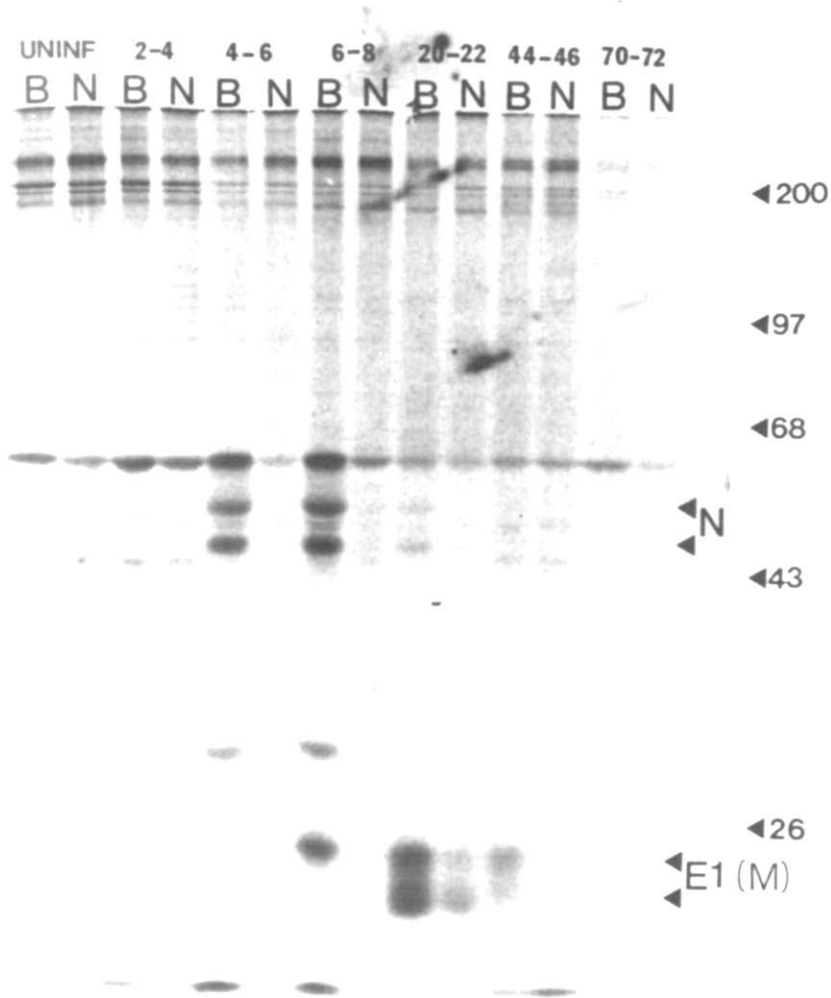


Fig. 4. Kinetics of synthesis of viral structural proteins. BCV-infected and uninfected BEK cells were pretreated with 2.5 $\mu\text{g}/\text{ml}$ of Actinomycin D 1 h prior to labeling with [^{35}S]methionine. After 2-h labeling at the indicated time points, cells were lysed and the lysates were immunoprecipitated with rabbit polyclonal antiserum against BCV virion structural proteins. The precipitates were electrophoresed on 10% polyacrylamide gels. B indicates proteins immunoprecipitated with an anti-BCV rabbit polyclonal antibody and N indicates proteins immunoprecipitated with a normal rabbit serum. Molecular weight markers in kilodaltons are indicated.

protein. At 20–22 h p.i., only a trace amount of proteins was being synthesized. Two virus-specific proteins in the molecular weight range 50–60 kDa were detected. These proteins most likely represent nucleocapsid protein (N). Also, two virus-specific proteins in the range of 20–30 kDa were detected, which are likely the

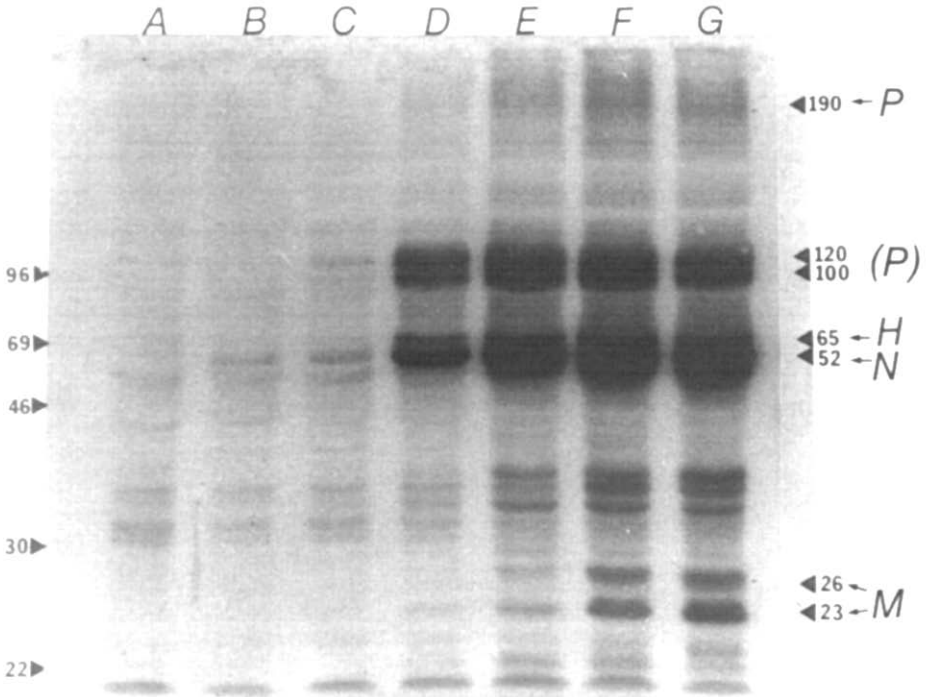


Fig. 5. Western blot analysis of BCV-specific structural proteins present in infected cells at different time points p.i. BCV-infected HRT cells were harvested at the indicated time points, electrophoresed on SDS-PAGE, transferred to nitrocellulose paper, incubated with a mixture of rabbit polyclonal and mouse monoclonal antibodies against virus structural proteins and then probed with [125 I]Protein A. Lanes A) uninfected; B) 4 h p.i.; C) 6 h p.i.; D) 8 h p.i.; E) 22 h p.i.; F) 46 h p.i.; G) 72 h p.i. Molecular weight markers in kilodaltons are indicated on the left of the figure.

various modified forms of M protein. The heterogeneity of N and M (E1) proteins has previously been noted in several other coronaviruses (Stern and Sefton, 1982; Robbins et al., 1986). Late in infection (between 20 and 46 h p.i.), a cellular protein also co-migrated with one of the M proteins (Fig. 4). The nature of this protein is unclear. The antibody used could not detect the P (E2) (gp 120–100) or H (E3) (gp 65) proteins (unpubl. data).

These results suggest that the viral subgenomic mRNAs are used for translation immediately following synthesis. The viral proteins synthesized probably form a pool, from which virus particles are assembled. To test this probability, the viral proteins synthesized at different time points in HRT and BEK cells were separated by polyacrylamide gel electrophoresis, transferred to a filter membrane and probed with a mixture of BCV-specific polyclonal and monoclonal antibodies. It is evident from Fig. 5 that viral proteins persist in BCV-infected HRT cells even late in infection. Similar results were obtained in either HRT or BEK cells (data not shown). It is notable that the H protein (gp 65) and the cleavage products of P

protein, p120 and p100, were detected by the Western blot technique (Fig. 5). The kinetics of accumulation of these proteins was similar to that of other BCV proteins. This result together with the data on the kinetics of protein synthesis (Fig. 4) indicates that sufficient viral proteins are synthesized early in infection and persist throughout replication cycle. Thus, the limiting component in BCV virus assembly could be the virion genomic RNA. Some proteins which migrated between N and M were also detected by immunoblotting. The nature of these proteins is not clear but may represent aggregates of M protein (Hogue et al., 1984).

Discussion

The data presented in this report indicate that the synthesis of subgenomic mRNAs and of genomic RNA in BCV-infected cells are differentially regulated. The subgenomic mRNAs are synthesized very early in infection, while the majority of genomic RNA is synthesized late. Since the peak of genomic RNA synthesis (40–72 h p.i.) coincides with the peak of maximum virus yield, it is likely that the genomic RNA synthesized late in infection represents the genomic RNA packaged into virus particles. Thus, this report is the first example of differential regulation of transcription and replication of coronavirus RNAs. It is not clear whether this differential regulation is characteristic of all coronaviruses. The previous failure to detect such differential regulation in other coronaviruses may be due to shorter replication cycles in those viruses. It should be noted that the genome-sized RNA contains two functionally different species that may or may not be structurally identical. One is the mRNA 1 which is presumably used for translation to produce RNA polymerase, and the other is the RNA destined for packaging into virions. It is probable that the genome-size RNA synthesized early in infection consists mainly of the mRNA 1 species which is required for production of RNA polymerase needed for subsequent RNA replication.

Our data also showed that the viral proteins are synthesized early in infection immediately following mRNA synthesis and accumulate throughout the replication cycle. Since the release of virus particles coincides with the synthesis of genomic RNA, it is likely that the rate-limiting step in BCV infection and particle assembly is the synthesis of genomic RNA. We cannot rule out, however, the possibility that synthesis of some nonstructural proteins or processing of a structural protein might also be differentially regulated and thus may also play a role in late virus assembly. Since we could not detect the synthesis of P or H proteins by immunoprecipitation, the role of these proteins in regulating virus assembly cannot be ruled out. However, the kinetics of the accumulation of these proteins is similar to other viral structural proteins (Fig. 5). Thus, it is reasonable to suggest that P and H proteins are also synthesized with the same kinetics as the other viral proteins.

The switching of BCV RNA synthesis from transcription of mRNAs to replication of genomic RNAs could involve the synthesis of a new polymerase or a new protein factor. In both cases of murine coronavirus and porcine transmissible gastroenteritis virus, the viral RNA polymerases detected late in the infection could

be separated into two distinct fractions (Brayton et al., 1982, 1984; Dennis and Brian, 1982). One of the two enzyme fractions of MHV codes for genomic RNA while the other codes for both genomic and subgenomic RNAs (Brayton et al., 1984). Temporal separation of these two activities was not investigated. The viral RNA polymerase activity in BCoV-infected cells has so far not been studied. It would be of interest to determine whether BCoV RNA polymerase activities could be separated into temporally regulated enzymatic fractions. Since the transcription of subgenomic mRNA species utilizes a discontinuous leader-primed transcription mechanism (Baric et al., 1985), which is different from the replication of genomic RNA, it is reasonable to suggest that the polymerases responsible for the synthesis of these two RNA species are different, or are modified forms of the same polymerase. It is not clear what proteins are responsible for such a switching or modification. Since the transcription and replication of BCoV RNA can be clearly separated, BCoV may provide a very useful system for studying the regulation of transcription and replication.

Although BCoV and MHV are related antigenically, their protein compositions differ in that BCoV contains an additional protein species, namely the hemagglutinin which is a 140 kDa glycoprotein composed of two 65 kDa subunits, that is not found in MHV. Consistent with this property is the presence of an additional (7 instead of 6) subgenomic RNA species in the BCoV-infected cells, which is not found in MHV-infected cells. This RNA has a molecular weight of approximately 3.1×10^6 . Since BCoV subgenomic mRNAs have a nested-set structure, the maximum coding capacity of this new RNA species should be the difference between the molecular weights of this RNA, 2a, and the next smaller mRNA (RNA 3, with a molecular weight of approximately 2.6×10^6). This size difference (0.5×10^6) corresponds to a coding capacity of approximately 430 amino acids. This value is comparable to the estimated protein backbone of the hemagglutinin (Hogue et al., 1984; King and Brian, 1982; King et al., 1985). Thus, it is likely that the mRNA 2a is the RNA encoding the hemagglutinin protein. However, this gene assignment will require confirmation from *in vitro* translation studies, which are currently infeasible because of the small quantity of intracellular RNAs available.

Acknowledgments

We would like to thank Drs. Stephen A. Stohlman, Lisa H. Soe, Susan C. Baker and Shinji Makino for helpful discussions. We would also like to thank Carol Flores for excellent typing of the manuscript. This work was supported by Public Health Research Grants AI 19244 (to M.M.C.L.) and AI 14367 (to D.A.B.).

References

- Baric, R.S., Stohlman, S.A., Razavi, M.K. and Lai, M.M.C. (1985) Characterization of leader-related small RNAs in coronavirus-infected cells: Further evidence for leader-primed mechanism of transcription. *Virus Res.* 3, 19-33.

- Brayton, P.R., Lai, M.M.C., Patton, D.F. and Stohlman, S.A. (1982) Characterization of two RNA polymerase activities induced by mouse hepatitis virus. *J. Virol.* 42, 847–853.
- Brayton, P.R., Stohlman, S.A. and Lai, M.M.C. (1984) Further characterization of mouse hepatitis virus RNA-dependent RNA polymerases. *Virology* 133, 197–201.
- Brian, D.A., Dennis, D.E. and Guy, J.S. (1980) Genome of porcine transmissible gastroenteritis virus. *J. Virol.* 34, 410–415.
- Callebaut, P.E. and Penseart, M.B. (1980) Characterization and isolation of structural polypeptides in hemagglutinating encephalomyelitis virus. *J. Gen. Virol.* 48, 193–204.
- Dennis, D.E. and Brian, D.A. (1982) RNA-dependent RNA polymerase activity in coronavirus-infected cells. *J. Virol.* 42, 153–164.
- Hirano, N., Fujiwara, K., Hino, S. and Matumoto, M. (1974) Replication and plaque formation of mouse hepatitis virus (MHV-2) in mouse cell line DBT culture. *Arch. Gesamte Virusforsch.* 44, 298–302.
- Hogue, B.G. and Brian, D.A. (1986) Structural proteins of human respiratory coronavirus OC43. *Virus Res.* 5, 131–144.
- Hogue, B.G., King, B. and Brian, D.A. (1984) Antigenic relationships among proteins of bovine coronavirus, human respiratory coronavirus OC43, and mouse hepatitis coronavirus A59. *J. Virol.* 51, 384–388.
- King, B. and Brian, D.A. (1982) Bovine coronavirus structural proteins. *J. Virol.* 42, 700–707.
- King, B., Potts, B.J. and Brian, D.A. (1985) Bovine coronavirus hemagglutinin protein. *Virus Res.* 2, 53–59.
- Laemmli, U.K. (1970) Cleavage of structural proteins during the assembly of the head of bacteriophage T4. *Nature* 227, 680–685.
- Lai, M.M.C. and Stohlman, S.A. (1978) The RNA of mouse hepatitis virus. *J. Virol.* 26, 235–242.
- Lai, M.M.C., Brayton, P.R., Armen, R.C., Patton, C.D., Pugh, C. and Stohlman, S.A. (1981) Mouse hepatitis virus A59: messenger RNA structure and genetic localization of the sequence divergence from the hepatotropic strain MHV3. *J. Virol.* 39, 823–834.
- Lai, M.M.C., Patton, C.D. and Stohlman, S.A. (1982) Replication of mouse hepatitis virus: negative-stranded RNA and replicative form RNA are of genome length. *J. Virol.* 44, 487–492.
- Lai, M.M.C., Patton, C.D., Baric, R.S. and Stohlman, S.A. (1983) Presence of leader sequences in the mRNA of mouse hepatitis virus. *J. Virol.* 46, 1027–1033.
- Lai, M.M.C., Baric, R.S., Brayton, P.R. and Stohlman, S.A. (1984) Characterization of leader RNA sequences on the virion and mRNAs of mouse hepatitis virus, a cytoplasmic virus. *Proc. Natl. Acad. Sci. USA* 81, 3626–3630.
- Lapps, W., Hogue, B.G. and Brian, D.A. (1987) Sequence analysis of the bovine coronavirus nucleocapsid and matrix protein genes. *Virology* 157, 47–57.
- Leibowitz, J.L., Wilhemsen, K.C. and Bond, C.W. (1981) The virus-specific intracellular RNA species of two murine coronaviruses: MHV-A59 and MHV-JHM. *Virology* 114, 39–51.
- Lomniczi, B. and Kennedy, I. (1977) Genome of infectious bronchitis virus. *J. Virol.* 24, 99–107.
- Makino, S., Taguchi, F. and Fujiwara, K. (1984) Defective interfering particles of mouse hepatitis virus. *Virology* 133, 9–17.
- McMaster, G.K. and Carmichael, G.G. (1977) Analysis of single- and double-stranded nucleic acids on polyacrylamide and agarose gels by using glyoxal and acridine orange. *Proc. Natl. Acad. Sci. USA* 74, 4835–4838.
- Robbins, S.G., Frana, M.F., McGowan, J.J., Boyle, J.F. and Holmes, K.V. (1986) RNA-binding proteins of coronavirus MHV: detection of monomeric and multimeric N Proteins with an RNA overlay-protein blot assay. *Virology* 150, 402–410.
- Spaan, W., Delius, H., Skinner, M., Armstrong, J., Rottier, P., Smeekens, S., van der Zeijst, B.A.M. and Siddell, S.G. (1983) Coronavirus mRNA synthesis involves fusion of noncontiguous sequences. *EMBO J.* 2, 1939–1944.
- Stern, D.F. and Kennedy, S.I.T. (1980) Coronavirus multiplication strategy. I. Identification and characterization of virus-specified RNA. *J. Virol.* 34, 440–449.
- Stern, D.F. and Sefton, B.M. (1982) Coronavirus proteins: structure and function of the oligosaccharides of the avian infectious bronchitis virus. *J. Virol.* 44, 804–812.
- Wege, H., Muller, A. and ter Meulen, V. (1978) Genomic RNA of the murine coronavirus JHM. *J. Gen. Virol.* 41, 217–228.